Characterizing Keratins Using High-Pressure Differential Scanning Calorimetry (HPDSC)

F.-J. WORTMANN and H. DEUTZ

Deutsches Wollforschungsinstitut an der TH-Aachen e.V. Veltmanplatz 8, D-51 Aachen, Germany

SYNOPSIS

Applying differential scanning calorimetry (DSC) for temperatures up to 180°C, the denaturation transition of the α-helical material of various keratins in excess water was studied at conditions of equilibrium water vapor pressure (high-pressure DSC). The results show a generally cystine content and material invariate denaturation range of 20–30°C with peak temperatures around 140°C. Though analysis of variance and multiple comparison tests show a pronounced inhomogeneity of the enthalpy data, the results generally support the material invariance of the denaturation enthalpy and hence of the helix content of the keratins. The denaturation enthalpy for the helical coiled-coil-structures in the intermediate filaments is determined as ΔH = 6.5–7.8 kJ/mol. A significant positive correlation was found between the denaturation temperatures and the cystine content. It is concluded, that the helix denaturation temperatures are kinetically controlled by the amount and/or the chemical composition of the surrounding nonhelical matrix, and that the double-peak endotherms observed for wool and other keratins originate from two cell types that are sufficiently different in sulfur content to allow endotherm separation. In the case of wool the cell types can be identified as "ortho-" and "paracortical" cells. © 1993 John Wiley & Sons, Inc.

INTRODUCTION

Materials made from hard keratin, namely hair, horn, nail, claw, hoof, and quill, exhibit a complex, morphological fine structure.[1] Judging from a purely mechanical point of view, the principle differences in the morphological components in α-keratins relate to their being either crystalline or amorphous. This has lead to the two-phase filament–matrix model for keratins, originally proposed by Feughelman.[2] In this model the helical fraction of the intermediate filaments, or microfibrils as they are called in the traditional terminology, can be identified as the crystalline, filamentous phase. The matrix in consequence contains summarily the rest of the morphological components, including cuticle, cell membrane complex, etc.[3,4]

Thermal analysis is especially suited to characterize the transitions of the phases of such a two-phase structure, namely, for the investigation of the glass transition and of the ageing and annealing behavior of the matrix phase[5,6] on the one hand and of the melting behavior of the α-helix on the other.[7–13] Though the melting of the α-helix in soluble proteins is, in the limiting case, a reversible, one-step, first-order transition,[14] the helix–coil transition is irreversible in the case of the insoluble keratins. For this reason the process will be referred to, in what follows, as denaturation rather than as a melting transition.

Using differential thermal analysis (DTA) and pressure resistant sample containers, Ebert et al.[10,15] investigated the transitions of wool fibers in various agents to study the phenomenon of supercontraction. For some of the conditions they applied, they observed multiple transitions at temperatures above approx. 100°C. Haly and Snaith[9] also used DTA to examine the performance of wool samples sealed into glass containers with various amounts of water. They observed a phase transition, often a doublet, that shifted with water content from approx. 230°C for dry wool to 140°C for wool in excess water.

More recently, Spei et al., as reviewed in Ref. 8, used differential scanning calorimetry (DSC) to investigate the denaturation behavior of various ker-

Journal of Applied Polymer Science, Vol. 48, 137–150 (1993)
 CCC 0021-8995/93/010137-14

atins in the dry state and proved[16] Astbury's[17,18] hypothesis of the strain-induced, molecular $\alpha \Leftrightarrow \beta$ transition in keratins. The peak Spei et al. detected at 240°C was attributed to the denaturation of the α-helical material, while a second peak, found in a doublet arrangement for some keratins at around 250°C, was attributed to matrix material (cystine decomposition) and was supposedly only observed for cystine-rich materials. Though Spei et al.[8,19] demonstrated that the denaturation peaks can usually adequately be detected and evaluated, it is obvious from their curves that the effect is always secondary in size compared to the background signal of their measurements that can be attributed to a general pyrolysis of the keratin.[11]

Taking advantage of the shift of the helix denaturation peak toward lower temperatures in water, Crighton and Hole[7] developed a measurement cell for high-pressure differential thermal analysis (HPDTA) to study the pronounced pressure dependence of the denaturation transition temperature of the helical material of various keratins in water, again in some cases appearing as a doublet, at temperatures around 140°C.

The aim of the present study was to examine in further detail the denaturation transition of the α-helical material in various keratins in excess water with respect to their chemical and morphological composition. Applying conventional DSC with pressure-resistant, commercially available steel capsules gave safe access to a temperature range up to 180°C (or even beyond) in which the denaturation transition temperatures as well as the enthalpies could be determined under conditions of equilibrium water vapor pressure.

EXPERIMENTAL

The following single samples of keratinous materials were investigated (sorted in order of increasing cystine content):

1. Rhinocerous horn (RH) from *Cerathotherium simus*
2. Porcupine quill (PQ) from *Hystrix cristata*
3. Mohair (MO)
4. Human finger nail (FN)
5. Merino wool (WO)
6. Echidna quill (EQ) from *Tachyglossus aculeatus*
7. Horse hair (HH)
8. Negroid hair (NH)

The mohair as well as the negroid hair originated from the United States. Merino wool was tested in the form of an unfinished fabric. The other samples originated from miscellaneous sources.

All DSC investigations were performed on a power-compensated DSC instrument (DSC-7, Perkin-Elmer), using pressure resistant (25 bar), stainless steel, large-volume capsules (Perkin-Elmer), and applying the following conditions:

Temperature range: 70–180°C
Heating rate: 5°C/min
Sample weight: 5–7 mg
Amount of added water: 50 μL

Prior to the measurement the samples were stored under constant, ambient room conditions (approx. 22°C, 55% RH) to ensure invariate water contents. Under these conditions a given material was weighed into the sample container, 50 μL of water was added and the container was sealed. An empty container without the O-ring rubber seal was used as reference.

The DSC instrument was calibrated prior to a given series of measurements, using indium and palmitic acid, both of high purity. In accordance with conventional practice in calorimetry, endothermic effects, i.e., heat absorption by the sample, are represented by an increase in the ordinate value from the baseline position.

Amino acid analyses were conducted by conventional methods on an LC 6000 Amino Acid Analyser (Biotronic). The results were found to be in good agreement with literature data.[7,11,20] The amino acid to be referred to in what follows is the double-amino-acid cystine, containing a disulfide crosslink. Its contents in the various keratins will be reported by referring to the mono-amino-acid, namely, to the molar fraction of cysteine residues (Cys-R, [mol %]). The expectation value for the 95% confidence limits of the Cys-R values is ±5% (relative).

Data analysis was conducted using Quattro Pro (Borland) and CSS:Statistica (Statsoft).

RESULTS

Figures 1–4 show HPDSC curves, redrawn from the originals, for mohair, finger nail, merino wool, and echidna quill. The figures were chosen to represent the general differences in the shapes and the locations of the peaks, though already the individual curves showed pronounced variations in their shapes and sizes. This observation, which has also been described by Spei and Holzem,[21] may either be attrib-

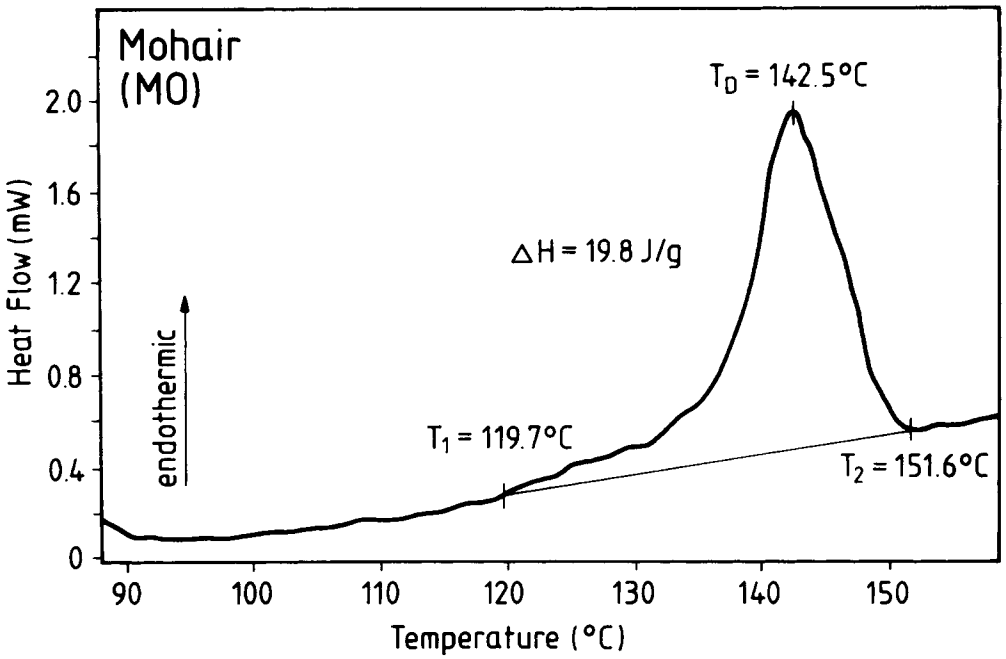

Figure 1 HPDSC trace for mohair (MO) under standard conditions (redrawn from the original). The relevant parameters of the curve are graphically defined.

uted to general, inherent, natural inhomogeneities of the samples, as reviewed by Marshall,[20] or to variations induced by the chemical and physical history of the samples. Namely, exposure to UV-light in the natural environment is known to reduce the amount of α-helical material detectable by DSC.[11,22,23]

For the samples consisting of comparatively fine fibers, namely, mohair, wool, and negroid hair, smooth DSC traces were observed. The traces generally exhibited an increased "roughness" for horse hair, as a very coarse fiber, and even more so for echidna and porcupine quill as bulk samples. A frequent observation, documented in Figure 4, is the

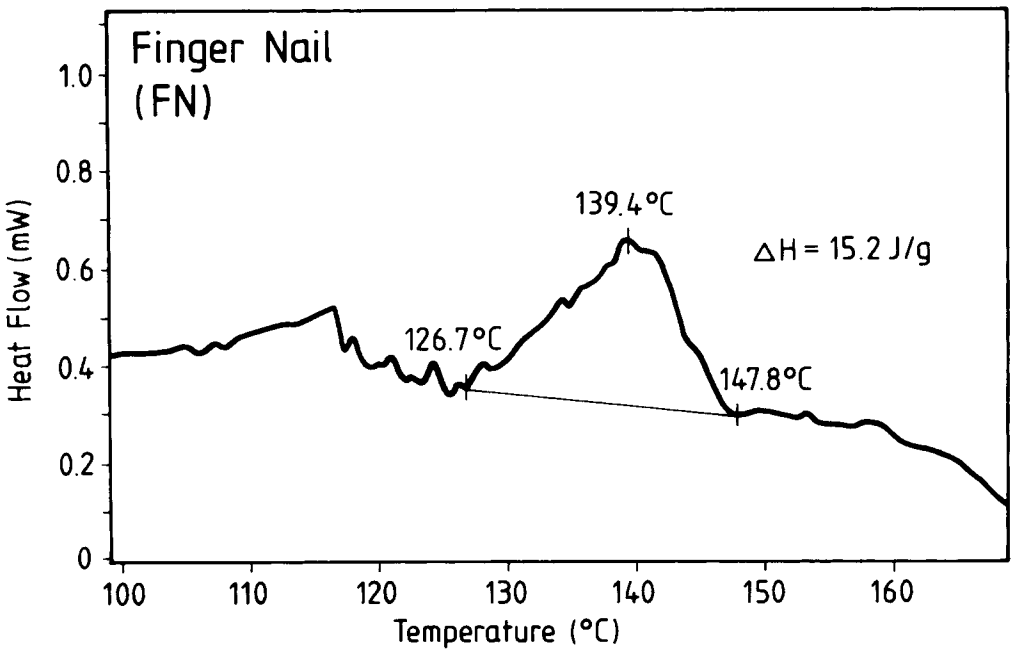

Figure 2 As Figure 1 but for finger nail (FN).

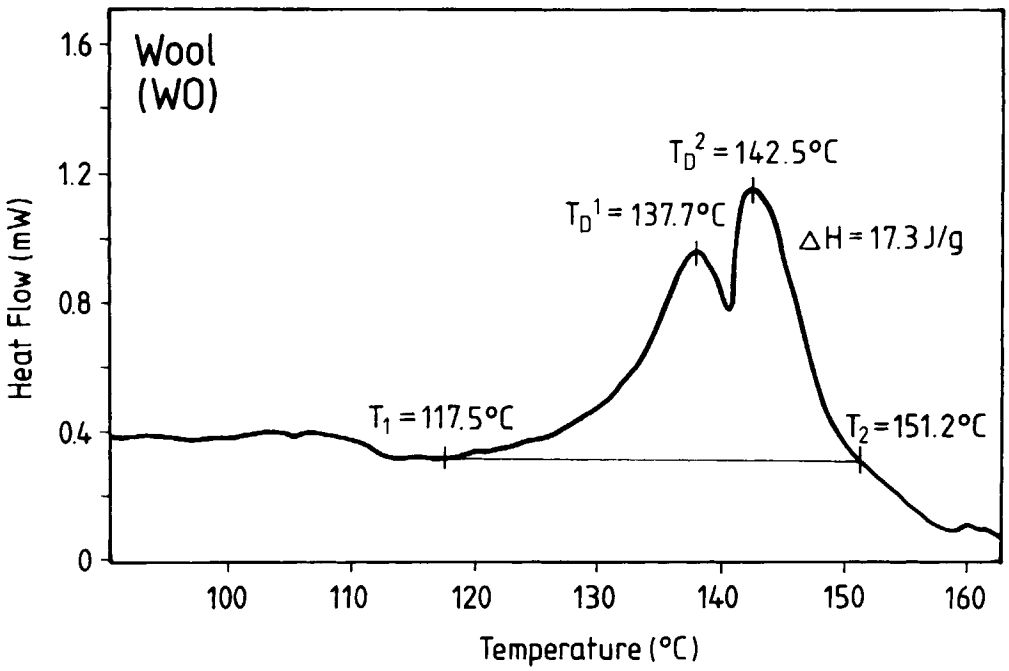

Figure 3 As Figure 1 but for merino wool (WO).

occurrence of a heat capacity change into the exothermal direction prior to the peaks for quill samples.

Figure 5 summarizes the individual results for the characteristic temperatures T_1 (start of the denaturation peak) and T_2 (end of the peak, see Fig. 1), which mark the range of the denaturation process. The results show a good reproducibility and, with the exception of rhinocerous horn (RH), a cystine and material invariate denaturation range of 24°C (SD = 4.3°C), that slightly shifts to higher temperatures with increasing cystine content.

In Figure 6 all individual results are summarized for the denaturation temperature T_D (see Fig. 1) of

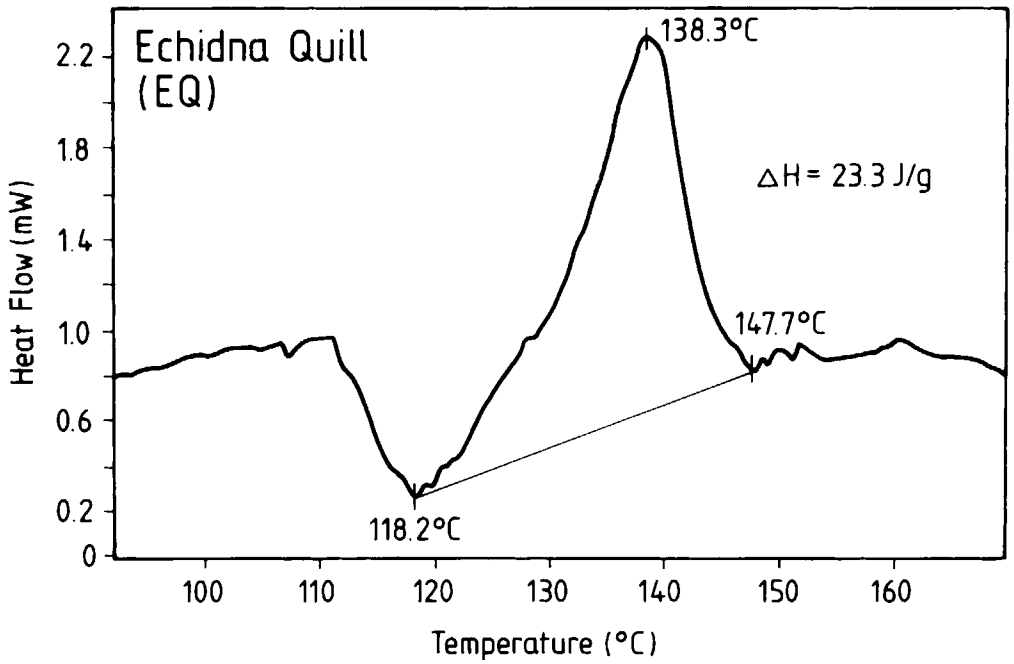

Figure 4 As Figure 1 but for echidna quill (EQ).

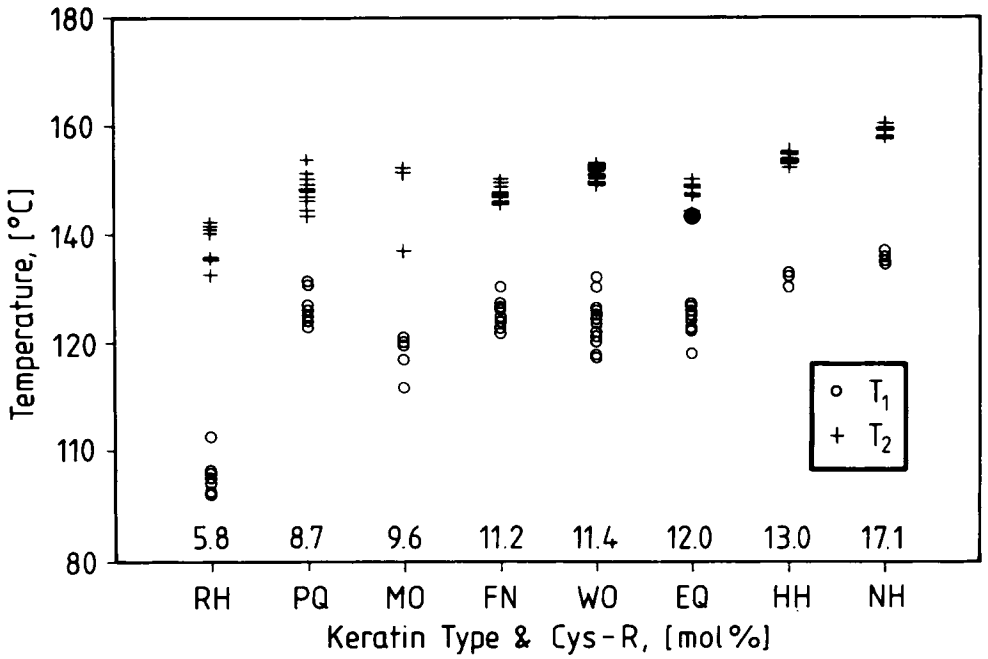

Figure 5 Individual results for the characteristic temperatures T_1 and T_2 (see Fig. 1), that mark the denaturation range for the various keratins, characterized by their contents of cystine residues.

the various keratins. The results show good reproducibilities and an increase of T_D with increasing cystine contents.

Variations from the single-peak structure toward a double-peak appearance, which have been observed by numerous investigators,[9,15,24,25] were observed for

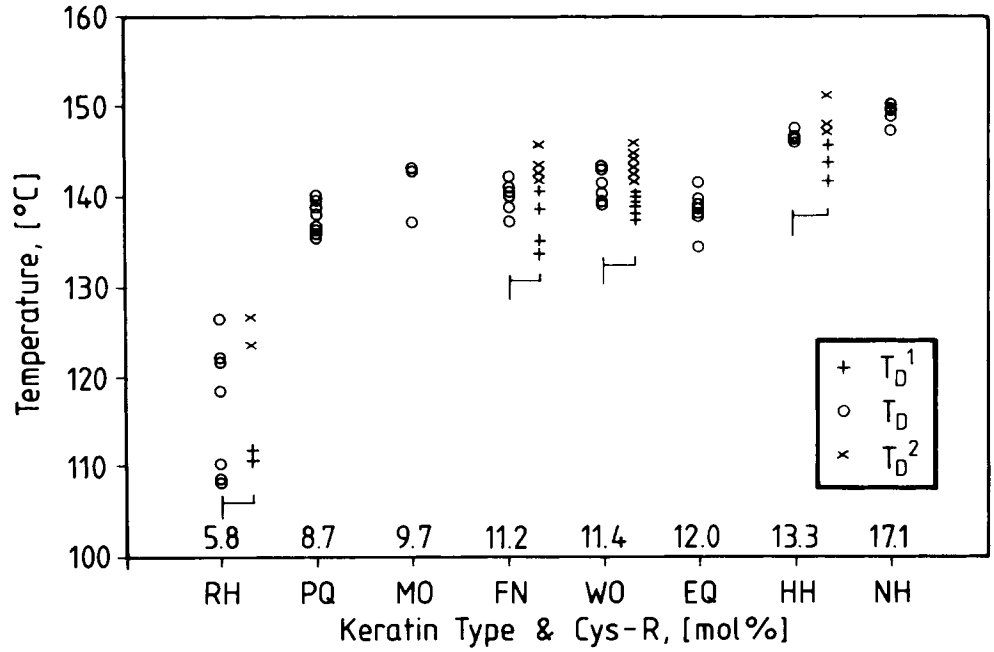

Figure 6 Individual results of the peak temperatures T_D for the various keratins, as characterized by their cystine contents. In cases of the appearance of double peaks, the characteristic temperatures T_D^1 and T_D^2 are offset along the x axis, as indicated, for reasons of clarity.

wool for roughly 70% of all measurements, where the separate peak temperatures T_D^1 and T_D^2 (see Fig. 3) are given in Figure 6. The tendency toward double peaks in the thermal spectrum was also observed, though considerably less pronounced, for finger nail (40%), horse hair (30%), and rhinocerous horn (20%). The difference between T_D^1 and T_D^2 is about 15°C for RH and on the average about 5°C for FN, WO, and HH.

For cases where single- as well as double-peak structures were observed in the thermograms, the peak temperatures for the single peak generally lay about half way between the double peaks, indicating two different processes of denaturation that express themselves with comparable intensity. Only in the case of rhino horn (RH) either one or the other process is favored (see Fig. 6), which may be attributed to the pronounced inhomogeneity of rhinocerous horn as a bulk material.[26]

Figure 7 summarizes the results for the denaturation enthalpies for the various keratins in the form of box-and-whisker plots, where the definitions of the graphical elements are given on the graph. Though there are pronounced variabilities of the experimental data, none of the results for a given material lay beyond the limits of three standard deviations around the individual mean, which would have made such a value suspect as an outlier. Table I summarizes the results for the denaturation enthalpies for the various keratins and their cystine contents.

The presentation of the data in Figure 7 shows that the denaturation enthalpies of the helical materials are independent of the cystine content and lack, with the possible exceptions of EQ and WO, pronounced differences for the various materials. To further investigate this aspect, analysis of variance (ANOVA) followed by multiple comparison was conducted. Emphasizing our interest in elucidating various aspects of the data with respect to homogeneity as well as to inhomogeneity, a conservative as well as a nonconservative test for multiple comparison were applied. The Tukey–HSD test is a test of medium conservativeness, while the LSD test offers the least amount of protection against erroneously finding significant differences.[27]

The results of ANOVA are summarized in standard form in Table II. They show the pronounced inhomogeneity of the data, where the group error (between groups) is more than nine times higher than the measurement error (within groups), leading to a severe rejection of the homogeneity hy-

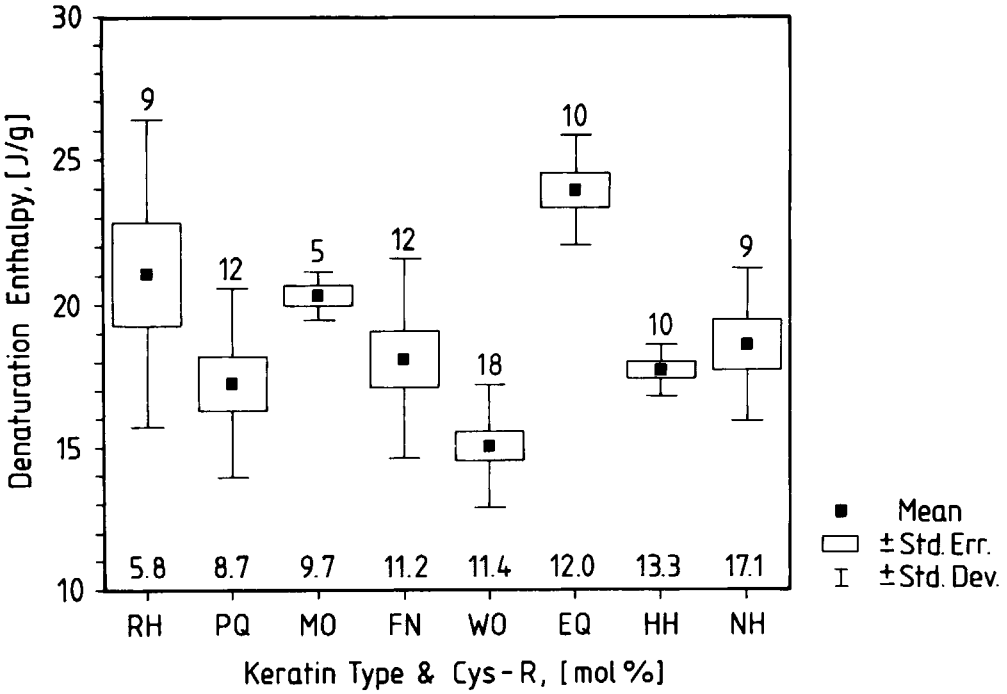

Figure 7 Box-and-whisker plot for the denaturation enthalpy results for the various keratins, identified by their labels and characterized by their cystine contents. The representation of means, standard deviations, and standard errors as graphical elements is defined in the legends. The digits above the individual plots give the number of measurements for each material.

Table I Cys-R Contents, Mean Denaturation Enthalpies (ΔH) and Their 95% Confidence Distances [q (95%)] for Various Keratins Sorted in Order of Increasing Enthalpies, the Grand Mean and Its Confidence Distance, and a Graphical Representation of the Results of the Multiple Comparison Analysis[a]

Label	Cys-R Content, mol %	ΔH (J/g)	q (95%)	Tukey HSD Test	LSD Test
WO	11.4	15.0	1.1	**	**
PQ	8.7	17.2	2.2	***	****
HH	13.3	17.7	0.7	***	***
FN	11.4	18.1	2.3	***	***
NH	17.1	18.5	2.2	***	****
MO	9.7	20.3	1.1	****	****
RH	5.8	21.1	4.4	***	**
EQ	12.0	23.9	1.4	**	*
All materials		18.4	0.9		

[a] See text.

pothesis. It is interesting to note that the F ratio is reduced to $F = 4.5$ (significance level 10^{-3}) if the data for EQ are omitted, and enters the range of homogeneity ($F = 1.7$, significance level 0.15) if the results for WO are taken out of the analysis. In the view of the significance levels that are observed for the various sets of data and taking into account the general robustness of ANOVA, the results are considered to be unaffected by the factual violation of the assumption of the homogeneity of variances, indicated in Figure 7.

Table I also summarizes the results of the multiple comparisons for the enthalpies of the different keratins in the form of rows of stars, each row representing a homogeneous group as identified by a given test procedure. The results of the two multiple comparison tests are consistent with those of ANOVA. The Tukey test emphasizes the homogeneity of the data, with only EQ, RH, and MO showing the tendency to form a high enthalpy group. The range of the homogeneous groups reflects the deviation from homogeneity for WO and even more so for EQ. The nonconservative LSD test very similarly accents the overall homogeneity of the majority of the materials, including WO, and only identifies EQ as an outlier.

DISCUSSION

The results of ANOVA and multiple comparison support the material invariance of the denaturation enthalpy for the majority if not all of the investigated keratins. Assigning the endothermic effects exclusively to the denaturation of the helical material leads to the conclusion that the helix content for these materials is largely invariate. A possible exception may be EQ that compared to the grand mean for the denaturation enthalpy of all other keratins, $\Delta H = 17.7$ J/g (SD = 3.6 J/g, $n = 75$), would have, on a relative basis, a 35% higher helix content than the other materials.

The results furthermore demonstrate the independence of the denaturation enthalpy and hence of the helix content from the cystine content of the materials. This is plausible, if not expected, in the view of the generally accepted material invariance of the structure of the intermediate filaments (IF) in keratins,[28] where the cystine of the keratin as a whole is mainly located outside the helical regions of the IFs, that is, in the nonhelical tails of the IF proteins and in all other matrix materials.

The large variations of the denaturation enthalpies and hence of helix contents that was observed

Table II Standard Representation for Results of Analysis of Variance on the Denaturation Enthalpy Data for Various Keratins, Leading to a Strong Rejection of Homogeneity Hypothesis

Source of Variation	Sum of Squares	DF	Mean Square	F Ratio	Sign. Level
Between groups	616.9	7	88.14	9.28	$< 10^{-5}$
Within groups	731.4	77	9.50		

by Spei et al.[8,25] for a variety of keratins, could not be confirmed. Assuming justifiably similar experimental variances for Spei's DSC results as for the present study (see Fig. 7), this would suggest that the differences in enthalpy and hence in crystallinity as shown, e.g., in Ref. 25, can mainly be attributed to natural measurement errors.

The variability in Spei's[25] data for the helix content can be further reduced toward homogeneity. This is achieved if the assumption that the second peak, which he observes for some keratins, is a "matrix" peak is dropped in favor of the assumption that the peaks relate to two types of α-helical material, which differ in thermal stability. This assumption is supported by Crighton's[24] observation that the introduction of additional crosslinks erases the double-peak resolution. The invalidity of the matrix peak hypothesis can furthermore be deduced from the fact that, though the occurrence of a peak doublet for a given material is an effect with a certain probability of occurrence (see Fig. 6), the enthalpy results remain unaffected by these variations of the endotherm structure.

The authors furthermore consider it rather difficult to envisage a morphological component in keratin, besides the α-helical material, that would be able to give a sharp endothermic effect, signifying a well-defined first-order transition. Even the hypothesis that the second peak relates to the melting of β-pleated sheet crystallites generated from the α-helical filaments (first peak of the doublet) was considered as unlikely by Haly and Snaith,[9] who originally proposed it.

In a recent summary of evidence originating from X-ray, infrared, and mechanical experiments, Feughelman[3] showed that keratin fibers contain a 25–30% fraction of material of the whole dry fiber that is impenetrable to water. This water-impenetrable phase has been identified as the crystalline, α-helical structure present in the IFs of keratin fibers.

Assuming for the present argument, and in agreement with literature results,[29] that the values of 25 and 30% mark the range for the amount of helical material for wool in general and specifically in the wool that was investigated in this study, the helix contents can be calculated for the other keratins on the basis of their denaturation enthalpies relative to that of wool. The results are summarized for the two cases (25 and 30% helix in dry wool) in Table III, together with literature data relating to X-ray diffraction measurements.[30] For the comparison between the experimental and the literature data the value of the helix content of human hair, probably originally determined for caucasian hair, was assumed to be also a good estimate for negroid hair (NH). The results in Table III show that the literature data for mohair and wool are well contained in the experimental data range, while the agreement appears to be unsatisfactory for horse hair (HH) and for negroid hair (NH).

Table III Helix Contents of Various Keratins Calculated From Their Denaturation Enthalpies Relative to That of Wool, Assuming 25 and 30% Helix Content, Respectively[a]

Type of Keratin	Helix Content on Basis		Literature Data (Ref. 13)
	25%	30%	
RH	35	42	
PQ	29	34	
MO	34	41	35
FN	30	36	
WO	25	30	30
EQ	40	48	
HH	30	35	25
NH	31	37	21
All materials	31	37	

[a] The results are compared with literature data.

The means and standard deviations of the enthalpies for the individual materials, as given in Figure 7, and for the keratins as a group (see Table I) allows one to calculate the ranges in which 95% of all enthalpy values are to be expected (mean $\pm$ 1.96 SD). Using these ranges and the two values of 25 and 30% helix in dry wool, respectively, the related helix content ranges are calculated and summarized in Figure 8. The comparison of the ranges with the literature data shows that they are in all cases either well contained or at least close to the DSC estimates.

Furthermore taking into account the correction procedures involved in X-ray crystallinity determinations,[29] the agreement between the DSC results and the X-ray data is considered to be satisfactory. This leads to the conclusion that the literature data for the helix contents in various keratins are consistent with the hypothesis of the material invariance of the helix content.

This result is in agreement with observations of Horikita et al.,[29] who determined by X-ray diffraction techniques helix crystallinities between 24 and 31% for different wools, various goat and cameloid hairs, and for angora rabbit hair, without detecting any significant material specific variations.

During our DSC experiments the keratins were

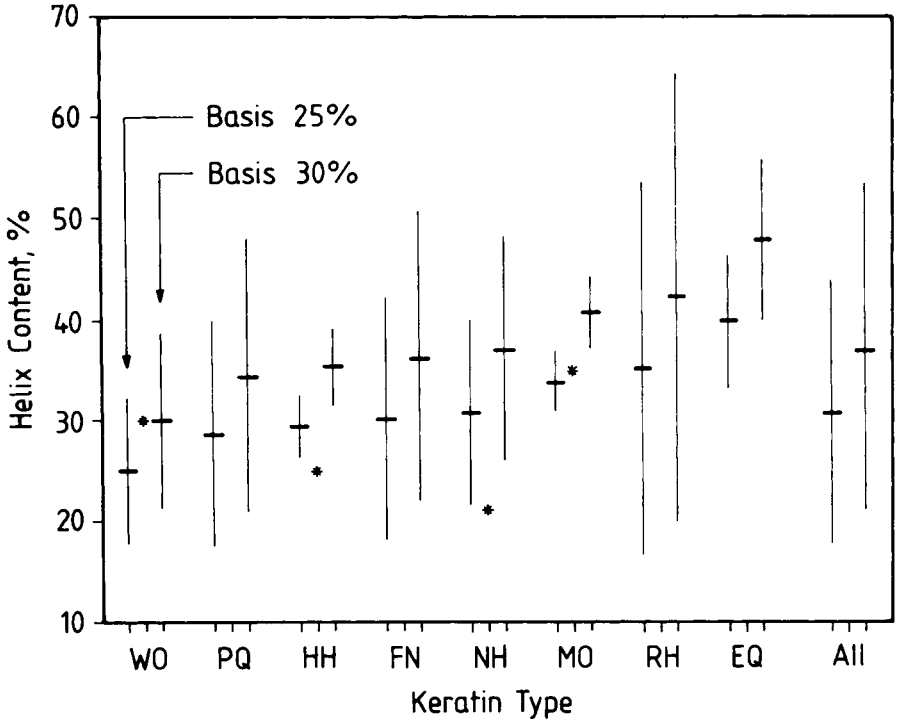

Figure 8 Helix content ranges calculated to include 95% of all experimental data for a given material. The ranges are based on enthalpy results and on the two cases of 25 and 30% helix in wool keratin, respectively. The means are given by the horizontal bars and the literature data by stars (*) (see text).

weighed into the sample containers at ambient room conditions (approx. 22°C, 55% RH). The water content of merino wool, related to the dry state, is approx. 14% under these conditions.[31] Correcting the mean denaturation enthalpy of merino wool (ΔH = 15.0 J/g, see Table I) for this water content gives ΔH = 17.1 J/g for dry wool. Since dry wool is assumed to be 25–30% helical,[3] a range of ΔH = 57.0–68.4 J/g is calculated for the denaturation enthalpy of the pure helical material in wool.

Taking into account the 95% confidence limits of roughly ±10% for the enthalpy of a given material (see Table I), and neglecting the error for the value of the water content, this range is in good agreement with the value of 40–65 J/g for the melting enthalpy of a similarly superstructured, fibrillar biopolymer, namely, collagen.[14]

It is generally accepted[28] that the IFs in keratins are formed by a fraction of proteins called low-sulfur (LS) proteins, which in purified form are about 63% α-helical.[32] Taking the amino acid analysis of this fraction, as determined by Marshall and Gillespie,[33] and calculating the weighed mean gives a molecular weight of 114 g/mol. This value leads to an estimated range for the denaturation enthalpy of α-helical material in keratin between ΔH = 6.5 kJ/mol and ΔH = 7.8 kJ/mol, on the basis of 30 and 25% α-helical material, respectively.

Considering the potential sources of inaccuracies, when estimating this range the results are in fair agreement with the value for the denaturation enthalpy of one residue in an isolated α-helix ΔH = 5 kJ/mol, as given by Privalov.[14] They also agree with the enthalpy for the transition of coiled-coil helices to the random-coil state in myosin, paramyosin, and tropomyosin fragments extrapolated to elevated temperatures (110°C), where the effects of hydrophobic interactions are removed, ΔH = 4.2–5.3 kJ/mol.[14]

The fact that the estimate for the denaturation enthalpy for the helical material in α-keratins turned out to be higher than Privalov's[14] results might furthermore suggest, in accordance with some data presented by Feughelman,[3] that an estimate of 30% helix (or more) rather than 25% for dry wool might be consistent with the experimental evidence for other helical biopolymers.

While the denaturation enthalpy turned out to be largely material invariate, a significant positive correlation was found between the denaturation temperatures and the cystine contents, in accordance with literature observations.[7,11] The results

are summarized in Figure 9 for those cases where only single peaks were observed. Regression analysis shows that for the majority of the keratins a linear model well describes the interrelation between the denaturation temperatures T_D and the cystine contents. The solid straight line in Figure 9 is based on the T_D values of all keratins, except RH, but extrapolated to include the RH data. Including the data for RH into the analysis, the coefficient of determination increases compared to a general linear model if a log-scale for the cystine content is used (see dotted line in Fig. 9). The restricted linear model yields a value for the increase of T_D with cystine content of 1.45°C/mol % Csy-R.

The denaturation enthalpy reflects the progress of the helix–coil transition in the crystalline sections of the intermediate filaments, where the concentration of cystine is low, and the location and distribution of the sulfur crosslinks are known to be material invariate.[28,34] The differences in the denaturation temperatures for the various keratins, as related to their cystine contents, must in consequence hence be attributed to the matrix, i.e., to the nonhelical parts of the IFs, to the material between the IFs, and to all other amorphous, morphological components. In this context it is interesting to note that Gillespie and Frenkel[35] observed a pronounced correlation between the cystine content of a keratinous material and its contents of high-sulfur proteins, which comprise the major fraction of the matrix material.

It has to be concluded that, though the denaturation enthalpy and the temperature range in which the denaturation takes place are material invariate, the thermal stability of the helical structures, i.e., the denaturation temperature, is controlled by the amount and/or the nature of the surrounding nonhelical matrix.

The following explanation for this phenomenon can be envisaged. When the helical sections in the intermediate filaments undergo the helix–coil transition, a major shape change for the molecular structures is the consequence, which macroscopically is observed as the phenomenon of supercontraction, that is, an approx. 25–50% contraction of the fiber.[36] This contraction induced by the helix–coil transition also imposes an affine deformation on the amorphous matrix phase in which it is embedded. The higher the crosslink density and/or the amount of matrix material, the more hindered the general shape change and hence the helix–coil transition will be, and the higher in consequence the

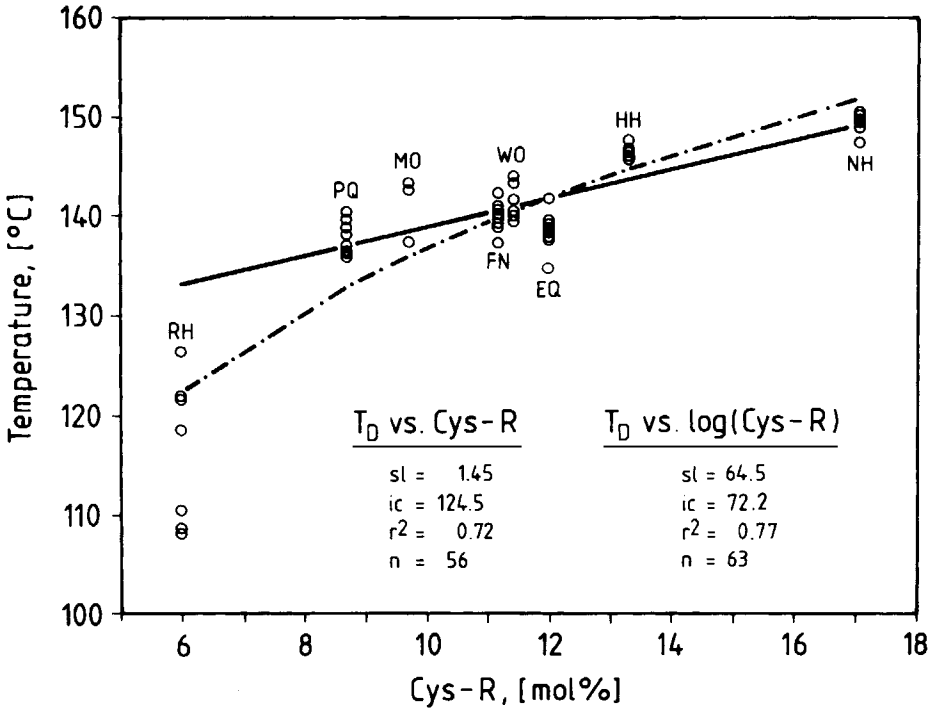

Figure 9 Regression analysis of the denaturation temperatures for single peak endotherms, examining T_D vs. Cys-R content for all keratins, safe RH (solid straight line), and T_D vs. log(Cys-R) for all materials (broken curved line). sl = slope, ic = y-axis intercept, r^2 = coefficient of determination, n = number of data points included in the analysis.

denaturation temperature in a constant heating rate experiment. This kinetic control of the location of the transition is confirmed by the pronounced heating rate dependence of T_D,[37] which is currently the subject of a detailed investigation.

Crighton et al.,[24] on analyzing the denaturation transition of various keratins using HPDTA under isobaric conditions observed a pronounced pressure dependence of T_D, which they attributed to the thermodynamics of the "melting" process, describable by the Clausius–Clapeyron equation. However, since the helix–coil transition can be considered to be roughly comparable to a solid–liquid transition, this would lead one to expect that T_D should show very little pressure dependence.[38] The fact that the change of T_D with pressure of 10–45°C/decade of pressure[24] is rather compatible with a solid–gas or liquid–gas transition than with a solid–liquid transition[38] again emphasizes the kinetic aspects of the helix denaturation.

These considerations lead to the consequence that the double-peak structure in the endotherm, observed quite frequently for wool and less frequently for other materials, is related to the denaturation of the helical fraction in intermediate filaments embedded in matrices of different cystine contents. The morphological components to satisfy this condition are readily identified for wool. As has first been shown by Horio and Kondo,[39] using differential dyeing techniques, merino wool contains two types of cells that are pronounced bilaterally arranged. The cell types differ in the arrangement of the filaments and in cystine contents.

The so-called paracortex shows a distinctly ordered, often hexagonal arrangement of filaments that are embedded in parallel to the fiber axis in a comparatively cystine-rich matrix. The orthocortex shows a "whorl-like" arrangement of the filaments, related to a systematic bias of the filament axes with respect to the fiber axis, embedded in a low-cystine matrix.[1] The overall Cys-R content is 8.7 mol % and 7.5 mol % for para- and orthocortical cells, respectively.[40]

Both of these values are lower than the Cys-R content found by Chapman and Bradbury[40] for their virgin wool (10.1 mol % Cys-R) and for the wool used in the current investigation (11.4 mol % Cys-R). This can be attributed to the comparatively high cystine content of the layer of cuticle cells that enclose only the fibrous keratins and make up a variable amount, but roughly 10% of the total fiber material. To compare the materials on a strictly uniform basis, corrections would need to be applied for the cuticle content of the fibrous keratins, shifting the data for MO, WO, HH, and NH to lower Cys-R contents. This would lead one to expect a somewhat higher value for the slope in the linear regression model (see Fig. 9).

The data for T_D^1 and T_D^2 of wool in Figure 6 show a mean difference of $\Delta T_D = 4.2$°C (SD = 0.8) between the denaturation temperatures of ortho- and paracortex. With the slope of the straight-line model in Figure 9 this would lead one to expect an approx. 3 mol % difference for Cys-R between the two cell types, leading with the value for Cys-R in wool in Table I to estimates of (11.4–1.5) = 9.9 mol % and (11.4 + 1.5) = 12.9 mol % Cys-R for ortho- and paracortex, respectively. While the overall higher Cys-R values for both cell types can be attributed to contributions of the cuticle, the difference of 3 mol % between the values is considerably higher than the difference of 1.2 mol % Cys-R found by Chapman et al.[40] However, the ratio of our DSC estimates for the Cys-R contents in para- and orthocortex 12.9/9.9 = 1.3 is lower than the ratio of the sulfur peak intensities $4.1 \times 10^3/2.6 \times 10^3 = 1.5$ determined in the macrofibrillar regions of the ortho- and paracortical cells in wool, applying scanning transmission electron microscopy (STEM) combined with energy dispersive X-ray analysis (EDX).[41]

First, considering the range of the individual temperature differences ΔT_D (see Fig. 6), second, plausibly assuming a nonperfect separation of ortho- and paracortical cells in Chapmann and Bradbury's experiment,[40] and third, considering the obviously high natural variability of a material like wool, the agreement between the various results obtained from HPDSC, cell separation,[40] and STEM/EDX[41] is considered to be satisfactory.

The results confirm the hypothesis, first mentioned by Haly et al.,[9] and recently again proposed by Crighton,[7,24] namely, that the endotherm doublet for wool and other keratins that show a bilateral structure, e.g., cashmere, is indeed related to the differential denaturation of the α-helical material in ortho/para cortex. From a more general point of view, also applicable for keratins without a distinct geometrical arrangement of two cell types, the occurrence of double-peak endotherms only requires the coexistence of two types of cells in a keratin in any given arrangement, for which the cystine contents are sufficiently dissimilar to lead to denaturation peaks differing enough in temperature to be resolved. Otherwise single peaks are observed that are located somewhere in the middle between the peaks for the pure components (see Fig. 6), depending on the size of their respective fractions.

The fact that all keratins show a comparable temperature range in which the denaturation pro-

Figure 10 Untreated merino wool fibers in the scanning electron microscope.

ceeds furthermore leads to conclude that all the keratins have a similar range of cells with different cystine contents, but double-peak structures only appear if in a given sample cell group differences in cystine content are pronounced enough to allow peak separation. This theory implies the assumption that, for a single cell the composition of the matrix material is homogeneous.

To investigate the consequence of the denaturation or rather of the partial denaturation on the macroscopical appearance of keratin fibers, wool samples were heated in the DSC just beyond the first denaturation peak and subsequently shock-cooled to room temperature. Figure 10 shows the typical, natural appearance of merino wool fibers and Figure 11 a fiber after the thermal treatment, which induced an effect to be named "differential supercontraction." It is quite obvious that due to a severe contraction only on the inside of the bent fiber a very strong crimp is introduced that has a much smaller radius of curvature than the natural crimp of the fibers. In addition it is known[42] that the orthocortex is generally located on the outside of the fiber crimp so that supercontraction of the orthocortex actually reverses the direction of the natural crimp. This phenomenon of differential supercontraction of wool fibers might be feasible to make use of in a technological process to impart new properties to wool fibers, e.g., for the use in high-bulk yarns.

To also study the effect of differential supercontraction for a keratin, which showed no tendency toward a peak doublet, negroid hairs were heated in the DSC up to the peak temperature, which is the point of approx. 50% helix–coil transition. The effects are, microscopically as well as macroscopically, much less spectacular than for wool. However, it was observed that the partial denaturation led to a reduction of the natural crimp, that is, to a straightening of the fibers. This initially led us to assume that the mechanism for negroid hair straightening is analog, though reverse, to that in wool, namely, that the fiber material on the outside of the natural crimp contracts and straightens the hair. This assumption had to be dropped during subsequent investigations, when no sign of a bilateral cortex structure could be found in the negroid hair samples, neither with TEM nor with SEM/EDX. In consequence it has to be concluded that though the partial supercontraction of the helical fraction in the IFs in negroid hair plays an important role for the hair straightening,[12] the mechanism by which this effect

Figure 11 SEM micrograph of a merino wool fiber, differentially supercontracted by HPDSC.

is generated is less specific than in the case of wool, where the interpretation in terms of ortho- and paracortex is straightforward.

The authors gratefully acknowledge the contributions made by Dr. J. Föhles (amino acid analysis) and by Mr. W. Arns (SEM). We are furthermore especially indebted to Dr. E. G. Bendit for generously providing the more exotic keratin samples. This work was supported by the Australian Wool Research Trust Fund, by the International Wool Secretariat, and also by the Ministerium für Wissenschaft und Forschung des Landes Nordrhein-Westfalen.

REFERENCES

1. R. D. B. Fraser, *Keratins: Their Composition, Structure, and Biosynthesis,* C. C. Thomas, Springfield, IL, 1982.
2. M. Feughelman, *Text. Res. J.,* **29,** 223 (1959).
3. M. Feughelman, *Text. Res. J.,* **59,** 739 (1989).
4. H. Zahn, U. Altenhofen, and F.-J. Wortmann, *"Wolle" Ullmans Encycl. Techn. Chem.,* **24,** 489 (1983).
5. D. G. Phillips, *Text. Res. J.,* **55,** 171 (1985).
6. M. G. Huson, *Polym. Internat.,* **26,** 157 (1991).
7. J. S. Crighton and E. R. Hole, *Proc. 7th Int. Wool Text. Res. Conf.,* **I,** 283 (1985).
8. M. Spei, *Melliand Textilber.,* **71,** 901 (1990).
9. A. R. Haly and J. W. Snaith, *Text. Res. J.,* **37,** 898 (1967).
10. G. Ebert, *Melliand Textilber.,* **48,** 87 (1967).
11. K. Jörissen, Ph.D. Thesis, RWTH, Aachen, 1982.
12. H. Deutz, F.-J. Wortmann, and H. Höcker, *Schriftenr. Dtsch. Wollf. Inst.,* **107,** 130 (1991).
13. W. D. Felix, M. A. McDowall, and H. Eyring, *Text. Res. J.,* **33,** 465 (1963).
14. P. L. Privalov, *Prot. Chem.,* **35,** 1 (1982).
15. G. Ebert and F. H. Müller, *Proc. Int. Wool Text. Res. Conf. CIRTEL Paris,* **4,** 487 (1965).
16. M. Spei, *Melliand Textilber.,* **72,** 202 (1991).
17. W. T. Astbury and A. Street, *Phil. Trans. Soc.,* **A230,** 75 (1931).
18. W. T. Astbury and H. J. Woods, *Phil. Trans. Soc.,* **A232,** 333 (1933).
19. M. Spei and R. Holzem, *Melliand Textilber,* **72,** 431 (1991).
20. R. C. Marshall in, J. Bereiter, A. G. Matoltsy, and K. S. Richards (Eds.), *Biology of the Integumen, Vol. 2, Vertebrates,* Springer-Verlag, Berlin, 1986, Chap. 35.
21. M. Spei and R. Holzem, *Colloid Polym. Sci.,* **265,** 965 (1987).
22. H. Deutz, G. Wortmann, and F.-J. Wortmann, Proc.

Int. Wool Text. Org. Conf. Techn. Cttee., Rep. Nr. 3, Lisbon (1991).
23. M. Spei and R. Holzem, *Melliand Textilber.*, **70,** 786 (1989).
24. J. S. Crighton, *Proc. 8th Int. Wool Text. Res. Conf. Christchurch NZ,* **I,** 419 (1990).
25. M. Spei and R. Holzem, *Colloid Polym. Sci.*, **267,** 549 (1989).
26. M. L. Ryder, *Turtox News,* **40,** 274 (1962).
27. CSS STATISTICA User Manual, Statsoft, Tulsa, OK (1991).
28. H. Zahn, *CHIMIA,* **42,** 289–297 (1988).
29. M. Horikita, M. Fukuda, A. Takaoko, and H. Kowai, *Sen-i Gakkaishi,* **45,** 367 (1989).
30. J. D. Turner and H. J. Woods, in, *Structure de la laine,* Inst. Text., France, 1961, p. 18.
31. I. C. Watt and R. L. D'Arcy, *J. Text. Inst.*, **70,** 298 (1979).
32. J. M. Gillespie in, L. A. Goldsmith (Ed), *Biochemistry and Physiology of Skin,* Oxford University Press, New York, 1983, p. 475.
33. R. C. Marshall and J. M. Gillespie, *Aust. J. Biol. Sci.*, **30,** 389–400 (1977).
34. L. G. Sparrow, L. M. Dowling, V. Y. Yoke, and P. M. Strike, in, G. E. Rogers, P. J. Reis, K. A. Ward, and R. C. Marshall (Eds.), *The Biology of Wool and Hair,* Chapman & Hall, London, 1988, p. 145.
35. J. M. Gillespie and M. J. Frenkel, *Comp. Biochem. Physiol. (B),* **47,** 339 (1974).
36. M. Feughelman, *Encycl. Polym. Sci. Eng.,* **8,** 566 (1987).
37. H. Deutz, F.-J. Wortmann, and H. Höcker, *Schriftenr. Dtsch. Wollf. Inst.,* **108,** 327 (1991).
38. P. W. Atkins, *Physical Chemistry,* 3rd ed., Oxford University Press, Oxford, 1986.
39. M. Horio and T. Kondo, *Text. Res. J.*, **23,** 373 (1953).
40. G. V. Chapman and J. H. Bradbury, *Arch. Biochem. Biophys.*, **127,** 157 (1968).
41. C. M. Carr, L. A. Holt, and J. Drennan, *Text. Res. J.*, **56,** 669 (1986).
42. G. Laxer and D. A. Ross, *Text. Res. J.*, **24,** 627 (1954).

Received April 3, 1992
Accepted June 8, 1992